Control of Smart Laminated FRP Structures using Artificial Neural Networks

Ankit Srivastava, Amit Agarwal, D. Chakraborty and A. Dutta

Journal of Reinforced Plastics and Composites 2005; 24; 1353 originally published online Jun 10, 2005;
DOI: 10.1177/0731684405049877

Control of Smart Laminated FRP Structures using Artificial Neural Networks

ANKIT SRIVASTAVA,[1] AMIT AGARWAL,[2] D. CHAKRABORTY[2,*] AND A. DUTTA[1]
[1]*Department of Civil Engineering*
[2]*Department of Mechanical Engineering*
Indian Institute of Technology
Guwahati, Assam, 781039, India

ABSTRACT: This paper deals with the vibration control of smart laminated fiber-reinforced plastic (FRP) composites using back propagation neural networks (BPNNs). To simulate the system dynamics, a finite element model for smart layered FRP composites is developed, which could incorporate any number of piezoelectric layers in addition to the usual composite layers. To control the vibrations of smart FRP laminated composites, BPNN has been used. Sensing and actuation are achieved by the piezoelectric sensors and actuators. The active vibration control performance of beams/plates with piezoelectric sensors and actuator layers is studied using this model. It has been observed that the use of neural network can control the displacement reasonably well.

KEY WORDS: laminated FRP composite, control, neural network, finite element method.

INTRODUCTION

FIBER-REINFORCED PLASTIC (FRP) composites are extensively used in aerospace, automobile, shipbuilding, and other industries due to their inherent advantages of lightweight, high strength to stiffness ratio along with the unique feature of tailor-made capability. Unlike the conventional materials, directional strength can be imparted to a composite component by the appropriate selection/design of stacking sequence. With the added characteristics, smart FRP composites with one or more piezoelectric sensor and actuator layers/patches have become an area of intensive research. Advanced structures with integrated self-monitoring and control capabilities are increasingly important due to the rapid development of space systems. This activeness of the structure is achieved by using smart materials. The basic feature of smart FRP laminates lies in its ability to actively control the vibration of structures. The layers/patches of smart materials act as sensors and actuators, which affect the controlling feature of the smart structures. The dynamic response of the smart laminated FRP structures can be easily generated using finite element analysis. The use of finite element for the analysis of dynamic behavior of piezoelectric actuated structure is an important area of research. Allik and Hughes [1] presented two finite element models in which isoparametric hexahedral and tetrahedral

*Author to whom correspondence should be addressed. E-mail: chakra@iitg.ernet.in

0731-6844/05/13 1353–12 $10.00/0 DOI: 10.1177/0731684405049877

elements were applied in a piezoceramic transducer design. However, the derived isoparametric elements were too thick for thin shell/plate applications. The thickness of substrate was almost equal to that of the piezoelectric layer. Tzou and Tsang [2], in 1989, presented a thin piezoelectric solid element with an internal degree of freedom (DOF). In 2000, Benjeddou [3] presented a survey of different piezoelectric solid finite elements that have been developed over the years. These elements have both structural and electrical DOFs. Some of these elements are eight-noded linear hexahedron, twenty-noded quadratic hexahedron, two-noded linear element, and three-noded quadratic elements. Liu et al. [4] developed a finite element model for the shape control and active vibration suppression of laminated composite plates with integrated piezoelectric sensors and actuators. The model is based on the classical laminated plate theory and the principle of virtual displacements.

Back Propagation Neural Network (BPNN) methods applied to control the smart FRP laminated composites is a recent area of research. Bailey and Hubbard [5] designed a distributed-parameter actuator and control theory. They used the angular velocity at the tip of a cantilever isotropic beam with constant-gain and constant-amplitude negative velocity algorithms and experimentally achieved vibration control. Gerhold and Rocha [6] used piezoelectric sensor–driver pairs that are collocated equidistant from the neutral axis for the active vibration control of free–free isotropic beams using constant-gain feedback control. Valoor et al. [7] used a self-adaptive neural network controller for the vibration control of the smart composite beams. The neural network identifier was trained offline using the data generated by the finite element model. Lee [8] used a neural network for system identification and control of smart structures. Three neural networks were developed, one for system identification, one for online state estimation, and the other for vibration suppression.

In this work, an eight-noded layered element has been developed, which can incorporate any number of composite layers along with the piezoelectric layers to act as sensors and actuators. The smart FRP laminates were modeled with these elements and the response of the smart laminates was obtained by 3D finite element analysis. The sensor voltage and the corresponding actuator voltages generated from the finite element analysis have been used to train a BPNN. The trained neural networks have been used as controllers, providing the actuator voltages as outputs necessary for displacement control. The testing and validation has been carried out for the neural network controller. Finally, the neural network is applied to control the vibrations of different structures.

FINITE ELEMENT ANALYSIS OF SMART LAMINATED FRP COMPOSITES

A layered 3D eight-noded solid element has been used for finite element modeling of the laminated plate. The shape functions of the element are:

$$N_i = \frac{1}{8}(1 + rr_i)(1 + ss_i)(1 + tt_i) \quad i = 1, 2, 3, \ldots, 8 \tag{1}$$

To adequately simulate the flexural response, extra shape functions have been introduced which are given by,

$$P_1 = (1 - r^2) \quad P_2 = (1 - s^2) \quad P_3 = (1 - t^2) \tag{2}$$

The displacement variation for an eight-noded solid element with incompatible modes is expressed as,

$$\{d\} = \begin{Bmatrix} u \\ v \\ w \end{Bmatrix} = \sum_{i=1}^{8} N_i \begin{Bmatrix} u_i \\ v_i \\ w \end{Bmatrix} + [P]\{\Psi\} \tag{3}$$

where,

$$[P] = \begin{bmatrix} P_1 & P_2 & P_3 & 0 & 0 & 0 & 0 & 0 & 0 \\ 0 & 0 & 0 & P_1 & P_2 & P_3 & 0 & 0 & 0 \\ 0 & 0 & 0 & 0 & 0 & 0 & P_1 & P_2 & P_3 \end{bmatrix} \tag{4}$$

$$[\Psi]^T = \begin{bmatrix} \Psi_1 & \Psi_2 & \Psi_3 & \Psi_4 & \Psi_5 & \Psi_6 & \Psi_7 & \Psi_8 & \Psi_9 \end{bmatrix}$$

$\Psi_1, \Psi_2, \ldots, \Psi_9$ are constants.

Variational principles are used to develop the finite element equations that incorporate the piezoelectric effect. The electromechanical constitutive equations for linear material behavior are given by,

$$\{T\} = [c]\{S\} - [e]\{E\} \tag{5}$$

$$\{D\} = [e]^T\{S\} + [\varepsilon]\{E\} \tag{6}$$

The equations presented here are the usual constitutive equations for structural and electrical fields, respectively, except for the coupling terms involving the piezoelectric matrix $[e]$. Here $\{T\}$ is the stress vector, $\{D\}$ is the electric flux density vector, $\{S\}$ is the strain vector, $\{E\}$ is the electric field vector, $[c]$ is the constitutive matrix, and $[\varepsilon]$ is the dielectric matrix.

Establishing nodal solution variables and element shape functions over an element domain, which approximates the solution, performs the finite element discretization.

$$\{u_c\} = [N^u]^T\{u\} \tag{7}$$

$$\{V_c\} = \left[N^V\right]^T\{V\} \tag{8}$$

Expanding these definitions, we get

$$\left[N^U\right]^T = \begin{bmatrix} N_1 & 0 & 0 & \cdots & N_n & 0 & 0 \\ 0 & N_1 & 0 & \cdots & 0 & N_n & 0 \\ 0 & 0 & N_1 & \cdots & 0 & 0 & N_n \end{bmatrix} \tag{9}$$

$$\left\{N^V\right\}^T = (N_1 N_2 \ldots N_n) \tag{10}$$

After the application of the variational principle and finite element discretization, the coupled finite element matrix equation derived for a one-element model is

$$\begin{bmatrix} [M][0] \\ [0][M] \end{bmatrix} \begin{Bmatrix} \{\ddot{u}\} \\ \{\ddot{V}\} \end{Bmatrix} + \begin{bmatrix} [C][0] \\ [0][C] \end{bmatrix} \begin{Bmatrix} \{\dot{u}\} \\ \{\dot{V}\} \end{Bmatrix} + \begin{bmatrix} [K]\left[K^Z\right] \\ \left[K^Z\right]^T\left[K^d\right] \end{bmatrix} \begin{Bmatrix} \{u\} \\ \{V\} \end{Bmatrix} = \begin{Bmatrix} \{F\} \\ \{L\} \end{Bmatrix} \tag{11}$$

where

$$[M] = \int_{\text{vol}} \rho[N^u][N^u]^T d(\text{vol}) \tag{12}$$

is the structural mass matrix

$$[K] = \int_{\text{vol}} [B^u]^T [C][B^u] d(\text{vol}) \tag{13}$$

is the structural stiffness matrix

$$\left[K^d\right] = -\int_{\text{vol}} [B_V]^T [\varepsilon][B_V] d(\text{vol}) \tag{14}$$

is the dielectric conductivity matrix

$$[K^z] = \int_{\text{vol}} [B_u]^T [e][B_V] d(\text{vol}) \tag{15}$$

is the piezoelectric coupling matrix; $\{F\}$ is the vector of nodal forces, surface forces, and body forces and; $\{L\}$ is the applied nodal charge vector.

Considering a laminate made up of N layers with a total thickness of T, the above equation is transformed as:

Structural stiffness:

$$[K] = \frac{2}{T} \int_{-1}^{1} \int_{-1}^{1} \sum_{k=1}^{N} \frac{t_k - t_{k-1}}{2} \int_{-1}^{1} G(r, s, t)\, dr\, ds\, dt \tag{16}$$

Dielectric conductivity:

$$\left[K^d\right] = \frac{2}{T} \int_{-1}^{1} \int_{-1}^{1} \sum_{k=1}^{N} \frac{t_k - t_{k-1}}{2} \int_{-1}^{1} G_1(r, s, t)\, dr\, ds\, dt \tag{17}$$

Piezoelectric coupling matrix:

$$[K^z] = \frac{2}{T} \int_{-1}^{1} \int_{-1}^{1} \sum_{k=1}^{N} \frac{t_k - t_{k-1}}{2} \int_{-1}^{1} G_2(r, s, t)\, dr\, ds\, dt \tag{18}$$

where

$$G(r, s, t) = [B_u]^T [C][B_u]|J|,$$
$$G_1(r, s, t) = -[B_v]^T [\varepsilon][B_v]|J|, \text{ and}$$
$$G_2(r, s, t) = [B_u]^T [e][B_v]|J|.$$

Then numerical integration for stiffness matrix has been evaluated using Gauss quadrature ($2 \times 2 \times 2$) scheme.

The generalized stiffness matrix is

$$\begin{bmatrix} [K] & [K^z] \\ [K^z]^T & [K^d] \end{bmatrix} \tag{19}$$

ARTIFICIAL NEURAL NETWORK-BASED CONTROLLER

Neural Network Architecture

As shown in Figure 1, artificial neural network (ANN) has a parallel and distributed processing structure. In general, it is composed of three layers: the input layer, the hidden layer, and the output layer. Each layer has a certain number of processing elements called neurons. Signals are passed between neurons over connection links. Each connection link has an associated weight, which, in a typical neural net, multiplies the signal transmitted. Each neuron applies an activation function (usually nonlinear) to its net input (sum of weighted input signals) to determine its output signal.

To build a model for the neural network controller, the network is processed through three stages: (1) The training stage, where the network is trained to predict output data based on the input data. (2) The testing stage, where the network is tested with a sample validation data set to check the accurate prediction of the neural network. (3) The evaluation stage, where the network ceases training and is used to control the active vibration of smart structures.

The training of the network by back propagation consists of three stages:

- feedforward of the input training pattern,
- calculation and backpropagation of the associated error, and
- weights adjustment.

Figure 1 shows a 2-2-1 (2 input nodes, 2 hidden nodes, and 1 output nodes) neural network. Here, inputs are denoted as I_1, I_2, and W_{ij} are the connection strengths or weights. Weights between input and hidden nodes are denoted by superscript h and those between hidden and output nodes are denoted by superscript o. Initially the weights are

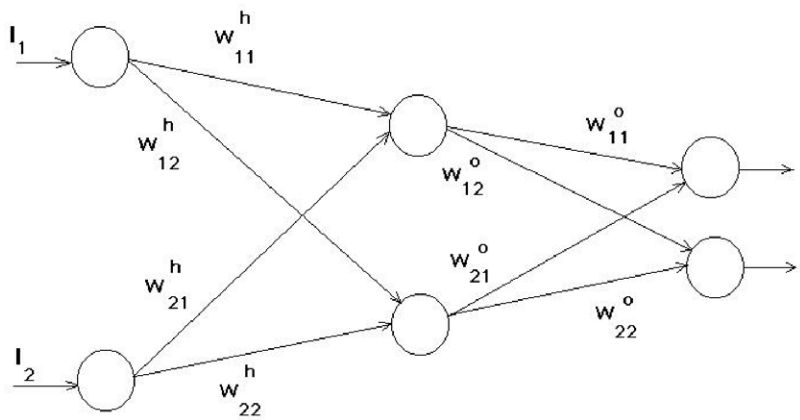

Figure 1. *Schematic diagram of a three-layer feed forward neural network.*

selected as random values between 0 and 1. Output from the hidden layer nodes are given as:

$$H_1 = \text{sgm}\left(\sum_{l=1}^{2} I_l W_{l1}^h\right) \tag{20}$$

$$H_2 = \text{sgm}\left(\sum_{l=1}^{2} I_l W_{l2}^h\right) \tag{21}$$

where, sgm( ) refers to the double sigmoidal function defined as:

$$\text{sgm}(x) = \left(\frac{2.0}{1+e^{-x}}\right) - 1 \tag{22}$$

Similarly, the output from the output nodes i.e., the final output of the network are given as:

$$O_1 = \text{sgm}\left(\sum_{m=1}^{2} H_m W_{m1}^o\right) \tag{23}$$

$$O_2 = \text{sgm}\left(\sum_{m=1}^{2} H_m W_{m2}^o\right) \tag{24}$$

which reduce to

$$O_1 = \text{sgm}\left(\sum_{m=1}^{2} \text{sgm}\left(\sum_{l=1}^{2} I_l W_{lm}^h\right) W_{m1}^o\right) \tag{25}$$

$$O_2 = \text{sgm}\left(\sum_{m=1}^{2} \text{sgm}\left(\sum_{l=1}^{2} I_l W_{lm}^h\right) W_{m2}^o\right) \tag{26}$$

For the purpose of training of the neural network, this output, is compared with the desired output, and the mean square error (MSE) is calculated. The modified weights are then calculated based on the value of the MSE. This procedure is repeated till the MSE becomes lesser than the desired value. The sample neural network architecture discussed here can be extended to any neural network with varying number of layers/nodes.

Implementation of Neural Network in Control

Back propagation neural network has been used for the control of the smart structures. A large number of finite element runs has been made and the sensor and actuator voltages are used to train the network. Sensor voltages have been used as input to the network and the corresponding actuator voltages have been used as the desired output. The number of neural networks that have been developed equals the number of actuator nodes for a particular problem. A single neural network, therefore, has one output and as many inputs as sensor nodes. Different combinations of learning rate and a number of hidden nodes have been tried, and depending upon the MSE and rate of convergence, the optimum network architecture is arrived at. Once the network is trained with the desired level of

error, it is tested with an unknown data set to check the validation of the network. Only after satisfactory performance of the network is it used to control the displacement of the plate.

RESULTS AND DISCUSSION

A $[0/45/-45/90]_{2s}$ graphite/epoxy cantilever beam subjected to load at free end having sensor and actuator layers made of piezoelectric materials has been considered in the present case. As shown in Figure 2, the following dimensions are used:

Length of the beam = 100 mm
Width of the beam = 50 mm
Thickness of the beam = 10 mm
Thickness of the piezo layer = 1 mm

The mechanical and electrical properties of materials are shown in Tables 1–3. For this problem, a large number of finite element simulations has been done and voltages of the sensor nodes and corresponding actuator nodes have been stored. Sample training data sets are listed in Table 4. BPNN has been trained with 500 such data sets and based on the MSE, the best architecture has been fixed. The sensor and actuator voltages were scaled

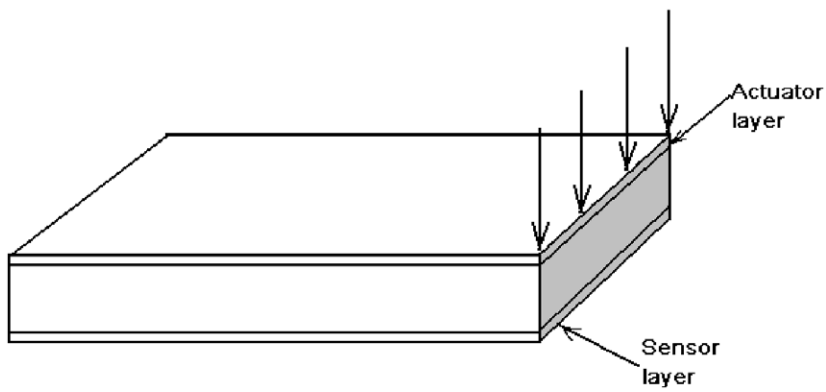

Figure 2. *Cantilever beam with full piezo layers.*

Table 1. Properties of graphite–epoxy composite.

	Modulus of elasticity (all in GPa)			Major Poisson's ratio	Other Poisson's ratio
Material	E_1	E_2	E_3	ν_{12}	ν_{23}
Graphite–epoxy	145.41	9.9974	9.9974	0.3	0.3

Table 2. Dielectric matrix.

	Dielectric matrix (in 10^{-9} F/m)			
Material	ε_{11}	ε_{22}	ε_{33}	$\varepsilon_{12}=\varepsilon_{13}=\varepsilon_{21}=\varepsilon_{23}=\varepsilon_{31}=\varepsilon_{32}$
PZT piezo	7.124	7.124	5.841	0

Table 3. Piezoelectric matrix.

	Piezoelectric matrix (in C/m^2)					
Material	e_{13}	e_{23}	e_{33}	e_{52}	e_{61}	$e_{11}=e_{12}=e_{21}=e_{22}=e_{31}=e_{32}=e_{41}=e_{42}=e_{43}=e_{51}=e_{53}=e_{62}=e_{63}$
PZT piezo	−4.1	−4.1	14.1	10.5	10.5	0

Table 4. Sample training data sets.

Data set 1		Data set 2		Data set 3		Data set 4	
Sensor voltage	**Actuator voltage**	**Sensor voltage**	**Actuator voltage**	**Sensor voltage**	**Actuator voltage**	**Sensor voltage**	**Actuator voltage**
−5.630e+7	−1.251e−3	8.296e+8	1.373e−3	1.480e+8	−1.464e−3	1.194e+9	1.556e−3
−6.579e+8	−5.635e−1	1.362e+8	8.916e−1	−5.849e+8	−2.196e−1	1.450e+8	5.476e−1
−1.423e+8	−1.932e−1	8.588e+8	7.384e−1	−3.420e+8	−2.836e−1	6.415e+8	8.288e−1
−5.488e+8	−8.087e−1	2.510e+8	5.430e−1	−3.501e+8	−2.774e−1	3.388e+8	1.177e−2
−4.006e+8	−5.849e−1	1.038e+9	8.997e−1	−4.691e+8	−2.145e−1	7.326e+8	5.293e−1
−2.684e+8	−4.798e−1	2.303e+8	5.996e−1	−3.407e+8	−7.195e−1	1.036e+8	8.393e−1
−5.508e+8	−3.502e−1	4.829e+8	4.452e−1	−3.946e+8	−5.402e−1	5.815e+8	6.352e−1
−2.768e+8	−8.959e−1	6.508e+8	8.066e−1	−4.095e+8	−7.172e−1	2.727e+8	6.279e−1
−1.527e+9	−8.228e−1	2.873e+8	3.266e−1	−1.568e+9	−8.305e−1	2.056e+8	3.344e−1
−1.751e+8	−7.465e−1	7.272e+8	5.589e−1	−2.617e+8	−3.713e−1	9.394e+8	1.837e−1
−5.039e+8	−1.741e−1	4.424e+8	1.695e−1	−5.893e+8	−1.650e−1	1.780e+7	1.605e−1
−4.281e+8	−8.589e−1	4.418e+8	8.602e−1	−3.289e+8	−8.616e−1	6.392e+8	8.629e−1
−9.106e+7	−7.104e−1	8.297e+8	3.861e−1	−1.185e+8	−6.173e−2	1.192e+9	7.373e−1
−6.370e+8	−5.135e−1	1.199e+8	1.849e−2	−5.599e+8	−5.234e−1	1.520e+8	2.838e−2
−1.454e+8	−3.039e−1	8.484e+8	9.812e−1	−3.286e+8	−6.585e−1	6.298e+8	3.357e−1
−5.395e+8	−1.498e−2	2.054e+8	5.440e−1	−3.288e+8	−7.321e−2	3.131e+8	6.023e−1
−4.323e+8	−9.140e−2	1.033e+9	9.098e−1	−4.882e+8	−7.282e−1	7.397e+8	5.466e−1
−2.562e+8	−3.644e−1	2.108e+8	9.267e−1	−3.202e+8	−4.890e−1	9.206e+7	5.133e−2
−5.475e+8	−1.473e−1	5.056e+8	2.031e−1	−4.001e+8	−2.590e−1	5.813e+8	3.149e−1
−2.601e+8	−1.658e−1	6.273e+8	8.838e−1	−3.943e+8	−6.017e−1	2.608e+8	3.196e−1
−1.536e+9	−9.884e−1	2.912e+8	3.368e−1	−1.564e+9	−6.852e−1	1.902e+8	3.363e−2
−1.866e+8	−4.456e−1	6.888e+8	9.181e−1	−2.773e+8	−3.905e−1	9.082e+8	8.630e−1
−5.140e+8	−1.190e−1	4.534e+8	5.773e−1	−6.056e+8	−3.552e−2	4.776e+6	4.937e−1
−4.070e+8	−4.669e−3	4.181e+8	2.187e−1	−3.060e+8	−4.328e−1	6.430e+8	6.468e−1

between −0.95 and 0.95 for the training of the BPNN. The training of the BPNN is continued till the MSE reaches 0.001. Various combinations of hidden node and learning rate have been tried in order to achieve minimum MSE for the networks. All the voltage corresponding to the sensor nodes are used as inputs and the voltage at one of the actuator nodes has been used as output to the BPNN. Therefore depending upon the number of actuator nodes, the number of BPNN to be trained will be different. Training MSE curve of the BPNN for one of the networks used is shown in Figure 3.

After the training phase, testing of the BPNN was done. The data, which the network had not seen before, were applied to the network for testing the network performance. To achieve this, a set of 100 different inputs was generated and fed to the already trained BPNN and the corresponding outputs were matched with the expected outputs generated from the finite element analysis. To show this validation of the neural network architecture, sample results of the testing phase are listed in Table 5.

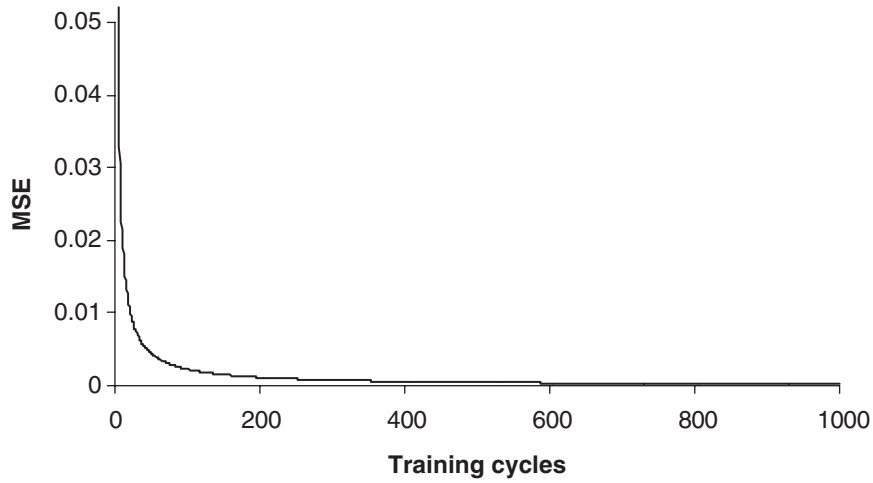

Figure 3. *Variation of mean square error (MSE) with training cycles.*

Table 5. Data set for testing of neural network.

Testing data set 1			Testing data set 2		
Sensor voltage	**Actuator voltage**	**NN Actuator voltage**	**Sensor voltage**	**Actuator voltage**	**NN Actuator voltage**
−2.021e+8	−1.647e−3	−1.636e−3	6.191e+8	1.770e−3	1.776e−3
−1.122e+9	−8.756e−1	−8.743e−1	1.456e+8	2.036e−1	2.043e−1
−1.334e+8	−3.739e−1	−3.753e−1	5.006e+8	9.191e−1	9.202e−1
−9.137e+8	−7.461e−1	−7.477e−1	3.662e+8	4.804e−1	4.813e−1
−8.815e+8	−8.441e−1	−8.445e−1	6.529e+8	1.588e−1	1.604e−1
−2.662e+7	−9.591e−1	−9.602e−1	6.681e+7	7.901e−2	7.914e−2
−9.305e+8	−7.301e−1	−7.322e−1	5.982e+8	8.251e−1	8.263e−1
−5.349e+7	−5.386e−1	−5.365e−1	2.763e+8	4.492e−1	4.488e−1
−1.265e+9	−8.383e−1	−8.393e−1	4.208e+8	3.422e−1	3.412e−1
−1.631e+8	−9.960e−1	−9.973e−1	6.620e+8	8.084e−1	8.072e−1
−3.434e+8	−1.560e−1	−1.547e−1	6.864e+7	1.515e−1	1.524e−1
−7.453e+8	−8.642e−1	−8.660e−1	5.698e+8	8.656e−1	8.668e−1
−1.804e+8	−4.129e−1	−4.150e−1	6.322e+8	8.862e−2	8.825e−2
−1.089e+9	−5.333e−1	−5.345e−1	1.484e+8	3.829e−2	3.845e−2
−1.285e+8	−1.300e−2	−1.312e−2	4.826e+8	6.902e−1	6.932e−1
−9.281e+8	−1.314e−1	−1.323e−1	3.405e+8	6.605e−1	6.608e−1
−8.959e+8	−3.650e−1	−3.672e−1	6.687e+8	1.835e−1	1.839e−1
−3.767e+7	−6.136e−1	−6.141e−1	6.372e+7	1.759e−1	1.771e−1
−9.138e+8	−3.707e−1	−3.723e−1	5.938e+8	4.266e−1	4.278e−1
−4.341e+7	−3.756e−2	−3.767e−2	2.587e+8	7.554e−1	7.553e−1
−1.266e+9	−3.819e−1	−3.820e−1	4.350e+8	7.303e−1	7.317e−1
−1.509e+8	−3.354e−1	−3.354e−1	6.292e+8	8.078e−1	8.034e−1
−3.504e+8	−9.519e−1	−9.511e−1	8.252e+7	4.101e−1	4.134e−1
−7.403e+8	−8.609e−1	−8.624e−1	5.655e+8	7.501e−2	7.502e−2

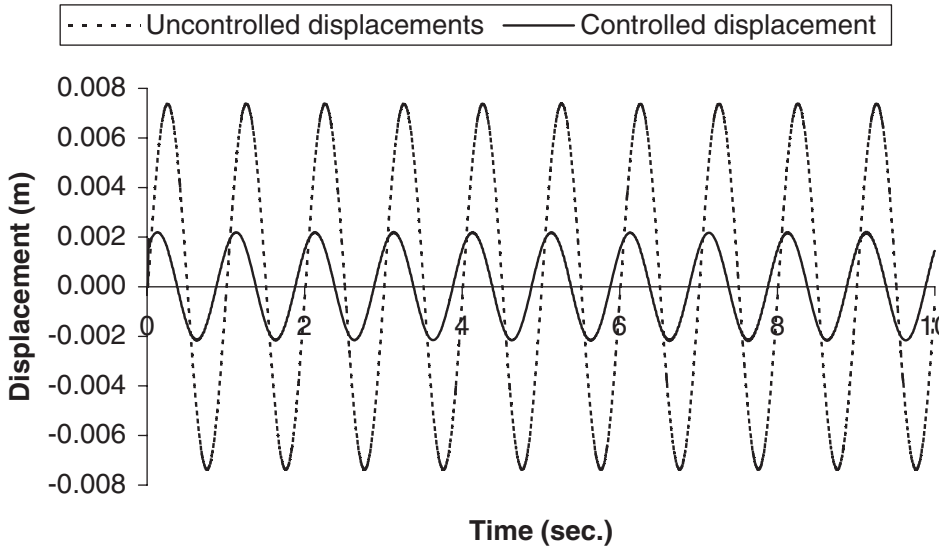

Figure 4. *Tip displacement with and without control for cantilever.*

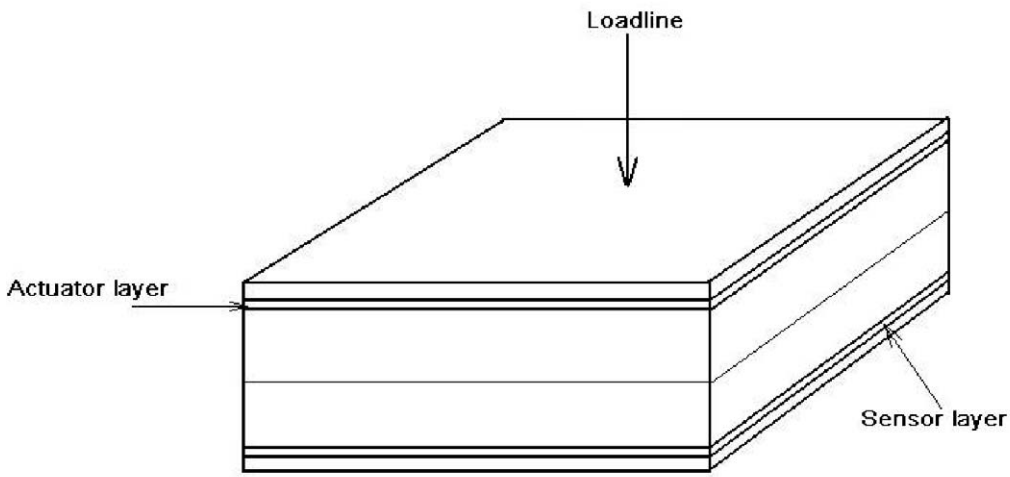

Figure 5. *Clamped Plate with piezo layers.*

These trained BPNNs are then used to control the displacement of the free end of the cantilever beam. A sinusoidal mechanical loading of 1000 N is applied uniformly at the free end. The uncontrolled and controlled tip displacements of the beam are shown in Figure 4. As shown in the figure, the neural networks could reduce the displacement by 70%.

For the next problem, a $[0/45/-45/90]_{2s}$ graphite/epoxy square plate subjected to load at the center having sensor and actuator layers made of piezoelectric materials has been considered. As shown in Figure 5, the following dimensions have been used:

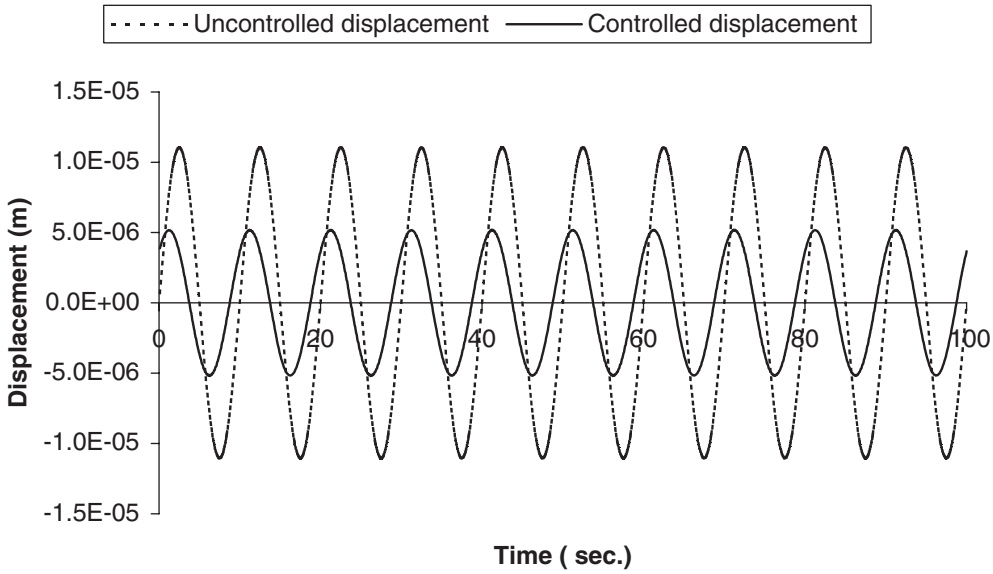

Figure 6. *Center displacement with and without control for clamped plate.*

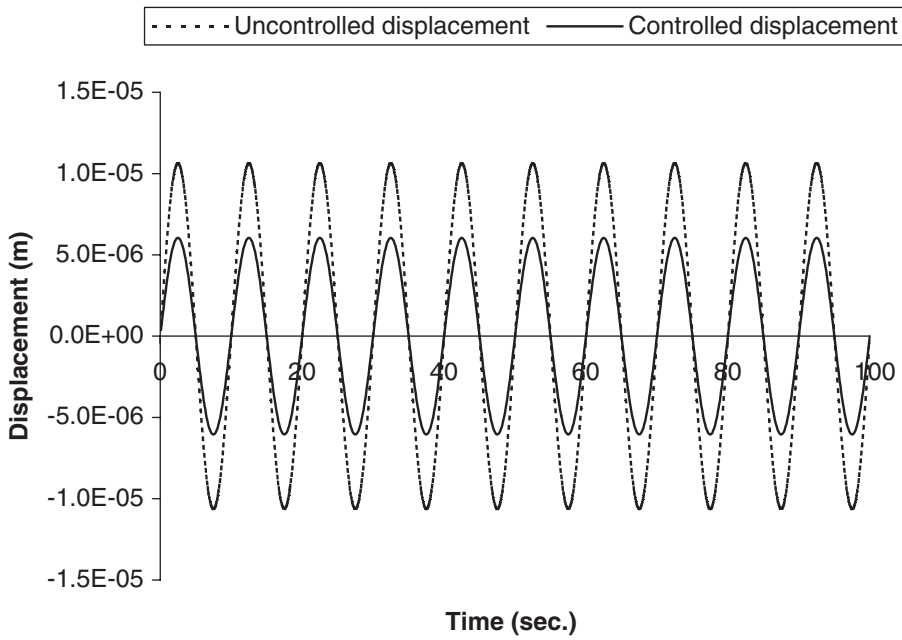

Figure 7. *Center displacement with and without control for simply supported plate.*

Length of the plate = 76.2 mm
Width of the plate = 76.2 mm
Thickness of the plate = 2.54 mm
Thickness of the piezo layer = 0.05 mm

In this case, the piezoelectric layers are embedded in the laminate. One smart layer is added after the top layer of the laminate, which acts as the actuator and another smart layer is added before the last layer of the laminate, which acts as the sensor. The above laminate with two different boundary conditions has been studied for the control of displacement using the BPNN. A sinusoidal mechanical loading is applied at the center of the plate. The controller based on BPNNs is applied to control the displacement of the plate. The same steps and methods were used to train the BPNN and use them for subsequent control of the network. Figure 6 shows the controlled and uncontrolled displacements for the plate clamped along all the four edges. It could be observed that the neural network-based controller is able to suppress the displacement up to 45% of the original plate center displacement. Figure 7 shows the controlled and uncontrolled displacement for the plate with simply supported boundary condition and subjected to the same sinusoidal loading at the center. The controlled displacement has been observed to be about 35% of the original plate displacement.

CONCLUSIONS

A layered solid element capable of incorporating any number of piezoelectric layers in addition to the usual FRP layers has been developed to carry out finite element analysis of smart laminated composites. The BPNN is trained and tested offline by using the data generated from the finite element analysis. It has been observed that the control methodology using the neural network can perform effectively in all the cases studied. In this work, finite element analysis simulation data have been used to train the neural network and for subsequent control of the laminates. However, experimentally generated data could be used to train the network and for better efficacy of the scheme.

REFERENCES

1. Allik, H. and Hughes, T. J. (1979). Finite Element Method for Piezoelectric Vibration, *Intl. J. of Numerical Methods in Engineering*, **2**: 151–168.
2. Tzou, H. S. and Tsang, C. I. (1990). Distributed Piezoelectric Sensor/Actuator Design for Dynamic Measurement/Control of Distributed Parameter Systems: A Finite Element Approach, *J. of Sound and Vibration*, **138**(1): 17–34.
3. Benejeddou, A. (2000). Advances in Piezoelectric Finite Element Modeling Adaptive Structural Elements: a Survey, *Computers and Structures*, **76**: 347–363.
4. Liu, G. R., Peng, X. Q. and Lam, K. Y. (1999). Vibration Control Simulation of laminated Composite Plates with Integrated Piezoelectrics, *J. of Sound and Vibration*, **220**(5): 827–846.
5. Bailey, T. and Hubbard, J. E. (1985). Distributed Piezoelectric-polymer Active Vibration Control of a Cantilever Beam. *J. Guidance, Control Dynam.*, **85**: 605–611.
6. Gerhold, C. H. and Rocha, R. (1989). Active Control of Flexural Vibrations in Beams, *J. Aerospace Eng.*, **23**: 141–154.
7. Manish, T., Valoor, K., Chandrashekhara and Agarwal Sanjeev (2001). Self Adaptive Vibration Control of Smart Composite Beams using Recurrent Neural Architecture, *J. of Solids and Structures*, **38**: 7857–7874.
8. Gwo Shiang Lee (1996). System Identification and Control of Smart Structures using Neural Networks, *Acta: Astronautica*, **38**(4–8): 269–276.